blood advances

American Society of Hematology
2021 L Street NW, Suite 900,
Washington, DC 20036
Phone: 202-776-0544 | Fax 202-776-0545
bloodadvances@hematology.org

BTK and PLCG2 remain unmutated in one third of patients with CLL relapsing on ibrutinib

Tracking no: ADV-2022-008821R1

Silvia Bonfiglio (Center for Omics Sciences, IRCCS Ospedale San Raffaele, Italy) Lesley-Ann Sutton (Karolinska Institutet, Sweden) Viktor Ljungström (Uppsala University, Sweden) Antonella Capasso (IRCCS Ospedale San Raffaele, Italy) Tatjana Pandzic (Uppsala University, Sweden) Simone Weström (Uppsala University, Sweden) Hassan Foroughi-Asl (Karolinska Institutet, Sweden) Aron Skaftason (Karolinska Institutet, Sweden) Anna Gellerbring (Clinical Genomics Stockholm, Science for Life Laboratory, Sweden) Anna Lyander (Clinical Genomics Stockholm, Science for Life Laboratory, Sweden) Francesca Gandini (IRCCS Ospedale San Raffaele, Italy) Gianluca Gaidano (University of Eastern Piedmont, Italy) Livio Trentin (University of Padua, Italy) Lisa Bonello (A.O.U Città della Salute e della Scienza, Italy) Gianluigi Reda (Fondazione IRCCS Cà Granda Ospedale Maggiore Policlinico, Italy) Csaba Bödör (HCEMM-SU Molecular Oncohematology Research Group, Hungary) Niki Stavroyianni (G. Papanicolaou Hospital, Greece) Constantine Tam (Peter MacCallum Cancer Centre and Department of Medicine, University of Melbourne, United States) Roberto Marasca (University of Modena e Reggio Emilia, Italy) Francesco Forconi (University Hospital National Health Service Trust, United Kingdom) Panayiotis Panayiotidis (National and Kapodistrian University of Athens, Greece) Ingo Ringshausen (University of Cambridge, United Kingdom) Ozren Jaksic (Dubrava University Hospital, Croatia) Anna Maria Frustaci (ASST Grande Ospedale Metropolitano Niguarda, Niguarda Cancer Center, Italy) Sunil Iyengar (Royal Marsden Hospital and Institute of Cancer Research, United Kingdom) Marta Coscia (A.O.U Città della Salute e della Scienza, Italy) Stephen Mulligan (Royal North Shore Hospital, Australia) Loïc Ysebaert (Institut Universitaire du Cancer de Toulouse-Oncopole, France) Vladimir Strugov (Almazov National Medical Research Centre, Russian Federation) Carolina Pavlovsky (FUNDALEU, Argentina) Renata Walewska (University Hospitals Dorset, United Kingdom) Anders Österborg (Karolinska Univeristy Hospital Solna, Sweden) Diego Cortese (Karolinska Institutet, Sweden) Pamela Ranghetti (san raffaele scientific institute, Italy) Panagiotis Baliakas (Science for Life Laboratory, Uppsala University, Sweden) Kostas Stamatopoulos (Institute of Applied Biosciences, Centre for Research and Technology Hellas, Greece) Lydia Scarfò (IRCCS Ospedale San Raffaele, Italy) Richard Rosenquist (Karolinska University Hospital, Sweden) Paolo Ghia (Università Vita-Salute San Raffaele, Italy)

Abstract:
Patients with chronic lymphocytic leukemia (CLL) progressing on ibrutinib constitute an unmet clinical need. Though BTK and PLCG2 mutations are associated with ibrutinib resistance, their frequency and relevance to progression are not fully understood. In this multicenter retrospective observational study, we analyzed 98 patients with CLL treated with ibrutinib (49 relapsing after an initial response and 49 still responding after {greater than or equal to}1 year of continuous treatment) using a next-generation sequencing (NGS) panel (1% sensitivity) comprising 13 CLL-relevant genes including BTK and PLCG2. BTK hotspot mutations were validated by droplet digital PCR (ddPCR) (0.1% sensitivity). By integrating NGS and ddPCR results, 32/49 relapsing cases (65%) carried at least 1 hotspot BTK mutation and/or PLCG2 mutation(s); in 6/32, BTK mutations were only detected by ddPCR [variant allele frequency (VAF) 0.1-1.2%]. BTK/PLCG2 mutations were also identified in 6/49 responding patients (12%; 5/6 VAF <10%), of whom 2 progressed at later time points. Among the relapsing patients, the BTK-mutated (BTKmut) group was enriched for EGR2 mutations, while BTK-wildtype (BTKwt) cases more frequently displayed BIRC3 and NFKBIE mutations. Using an extended capture-based panel, only BRAF and IKZF3 mutations showed a predominance in relapsing cases, who were enriched for del(8p) (n=11; 3 BTKwt). Finally, no difference in TP53 mutation burden was observed between BTKmut versus BTKwt relapsing cases, and ibrutinib treatment did not appear to favor selection of TP53-aberrant clones. In conclusion, we show that BTK/PLCG2 mutations were absent in a substantial fraction (35%) of a real-world cohort failing ibrutinib, and propose additional mechanisms contributing to resistance.

Conflict of interest: COI declared - see note

COI notes: G.G.: advisory board/speaker's bureau: Janssen, Abbvie, AstraZeneca, Beigene. F.F.: honoraria/advisory board: AbbVie, Acerta/AstraZeneca, Janssen-Cilag, BC platforms. O.J.: consultancy: AstraZeneca, Eli Lilly; speaker's bureau: Abbvie, AstraZeneca, Johnson and Johnson. R.W.: meeting sponsorship: AbbVie, Janssen; advisory board: AstraZeneca, Janssen, SecuraBio, Abbvie; speaker: AbbVie, AstraZeneca, Janssen, Beigene. A.O.: research funding: Beigene, Janssen, AstraZeneca and Gilead. P.B.: honoraria: Abbvie, Gilead, and Janssen; research funding: Gilead. K.S.: honoraria/advisory board: AbbVie, Acerta/AstraZeneca, Gilead, Janssen; research funding: AbbVie, Gilead, Janssen. L.S.: advisory board: AbbVie, AstraZeneca, Janssen. R.R.: honoraria/advisory board: Abbvie, AstraZeneca, Janssen, Illumina and Roche. P.G.: honoraria/advisory board: AbbVie, Acerta/AstraZeneca, Adaptive, ArQule/MSD, BeiGene, CelGene/Juno, Gilead, Janssen, Loxo/Lilly, Sunesis; research funding: AbbVie, Gilead, Janssen, Novartis, Sunesis. The other authors declare no competing financial interests.

Preprint server: No;

Author contributions and disclosures: S.B. coordinated sample collection, performed NGS experiments, interpreted data and wrote the paper; L.A.S. performed NGS experiments, interpreted data and wrote the paper; V.L. performed bioinformatics analysis and wrote the paper; A.C. analyzed and interpreted clinical data; T.P. and S.W. performed ddPCR experiments and analysis; H.F. and A.S. performed bioinformatic analysis on the lymphoid panel data; A.G. and A.L. prepared and sequenced libraries for the lymphoid panel; F.G. interpreted lymphoid panel data and wrote the paper; P.R. performed sample purification and DNA extraction; L.S. designed the study, coordinated clinical data collection, analyzed and interpreted clinical data and wrote the paper; P.G. and R.R. designed the study, interpreted data and wrote the paper; all authors provided samples and clinical data, and edited and approved the paper for submission.

Non-author contributions and disclosures: No;

Agreement to Share Publication-Related Data and Data Sharing Statement: NGS data for HaloPlex (fastq files) have been deposited to the European Nucleotide Archive (ENA), https://www.ebi.ac.uk/ena/ (accession ID PRJEB44894). Lymphoid panel NGS data (CRAM files) access is available via Figshare at https://doi.org/10.17044/scilifelab.19721998

Clinical trial registration information (if any):

BTK and *PLCG2* remain unmutated in one third of patients with CLL relapsing on ibrutinib

Silvia Bonfiglio[1,2*], Lesley-Ann Sutton[3*],Viktor Ljungström[3,4*], Antonella Capasso[5], Tatjana Pandzic[4], Simone Weström[4], Hassan Foroughi-Asl[3], Aron Skaftason[3], Anna Gellerbring[6,7], Anna Lyander[6,7,8], Francesca Gandini[2,9], Gianluca Gaidano[10], Livio Trentin[11], Lisa Bonello[12,13], Gianluigi Reda[14], Csaba Bödör[15,16], Niki Stavroyianni[17], Constantine S. Tam[18], Roberto Marasca[19], Francesco Forconi[20,21], Panayiotis Panayiotidis[22], Ingo Ringshausen[23], Ozren Jaksic[24], Anna Maria Frustaci[25], Sunil Iyengar[26], Marta Coscia[13,27], Stephen P. Mulligan[28], Loïc Ysebaert[29], Vladimir Strugov[30], Carolina Pavlovsky[31], Renata Walewska[32], Anders Österborg[33], Diego Cortese[3], Pamela Ranghetti[2], Panagiotis Baliakas[4], Kostas Stamatopoulos[34], Lydia Scarfò[2,5,9§], Richard Rosenquist[3,35§], and Paolo Ghia[2,5,9§]

[1]Centre for Omics Sciences, IRCCS Ospedale San Raffaele, Milan, Italy; [2]B cell Neoplasia Unit, Division of Experimental Oncology, IRCCS Ospedale San Raffaele, Milan, Italy; [3]Department of Molecular Medicine and Surgery, Karolinska Institutet, Stockholm, Sweden; [4]Department of Immunology, Genetics and Pathology, Science for Life Laboratory, Uppsala University, Sweden; [5]Strategic Research Program on CLL, IRCCS Ospedale San Raffaele, Milan, Italy; [6]Clinical Genomics Stockholm, Science for Life Laboratory, Solna, Sweden; [7]Department of Microbiology, Tumor and Cell Biology, Karolinska Institutet, Stockholm, Sweden; [8]School of Engineering Sciences in Chemistry, Biotechnology and Health, KTH Royal Institute of Technology, Stockholm, Sweden. [9]Università Vita-Salute San Raffaele, Milan, Italy; [10]Division of Hematology, Department of Translational Medicine, University of Eastern Piedmont, Novara, Italy; [11]Hematology and Clinical Immunology, Department of Medicine, University of Padua, Italy; [12]Molecular Pathology Unit, A.O.U Città della Salute e

della Scienza, Torino, Italy; [13]Department of Molecular Biotechnologies and Health Sciences, Università di Torino, Italy; [14]Hematology Department, Foundation IRCCS Ca' Granda Ospedale Maggiore Policlinico, Milan, Italy; [15]HCEMM-SU Molecular Oncohematology Research Group, Budapest, Hungary; [16]1st Department of Pathology and Experimental Cancer Research, Semmelweis University, Budapest, Hungary; [17]Hematology Department and HCT Unit, G. Papanicolaou Hospital, Thessaloniki, Greece; [18]Hematology Department, Peter MacCallum Cancer Centre and Department of Medicine, University of Melbourne, Melbourne, Australia; [19]Hematology Unit, Department of Medical and Surgical Sciences, University of Modena and Reggio Emilia, Modena, Italy; [20]School of Cancer Sciences, Faculty of Medicine, University of Southampton, Southampton, UK; [21]Hematology Department, University Hospital National Health Service Trust, Southampton, UK; [22]Department of Propaedeutic Internal Medicine, Laiko Hospital, University of Athens, Athens, Greece; [23]Department of Hematology, University of Cambridge, Cambridge, United Kingdom; [24]Dubrava University Hospital, Zagreb, Croatia; [25]Department of Hematology, Niguarda Cancer Center, ASST Grande Ospedale Metropolitano Niguarda, Milano, Italy; [26]Department of Haemato-Oncology, Royal Marsden Hospital, London, UK; [27]Division of Hematology, A.O.U. Città della Salute e della Scienza, Torino, Italy; [28]Royal North Shore Hospital, University of Sydney, Sydney, Australia; [29]Département d'Hématologie, Institut Universitaire du Cancer-Oncopole de Toulouse, Toulouse, France; [30]Almazov National Medical Research Centre, St Petersburg, Russia; [31]FUNDALEU, Clinical Research Center, Buenos Aires, Argentina; [32]Department of Molecular Pathology, University Hospitals Dorset, Bournemouth, UK; [33]Department of Hematology, Karolinska University Hospital, Stockholm, Sweden; [34]Institute of Applied Biosciences, Centre for Research and Technology Hellas, Thessaloniki, Greece; [35]Clinical Genetics, Karolinska University Hospital, Stockholm, Sweden.

*Shared first authors; §Shared last authors

Running title: Ibrutinib resistance in CLL

Corresponding author:

Paolo Ghia, MD PhD, Università Vita Salute San Raffaele, Milan, Italy, **ghia.paolo@hsr.it**

Phone number: +39-0226434797; Fax number: +39-0226432611

Abstract word count: 250 words

Text word count: 4133 words

Figure/table count: 2 figures; 3 tables

Reference count: 33

Article type: regular article

Data Sharing Statement

NGS data for HaloPlex (fastq files) have been deposited to the European Nucleotide Archive (ENA), https://www.ebi.ac.uk/ena/ (accession ID PRJEB44894), while lymphoid panel NGS data (CRAM files) is available via Figshare at https://doi.org/10.17044/scilifelab.19721998.

Key points

- One third of patients with CLL relapsing on ibrutinib do not carry *BTK/PLCG2* mutations, even with a 0.1% sensitivity.
- Additional mechanisms, such as del(8p), *EGR2* and NF-κB pathway mutations, may be cooperating in determining progression on ibrutinib.

Abstract

Patients with chronic lymphocytic leukemia (CLL) progressing on ibrutinib constitute an unmet clinical need. Though *BTK* and *PLCG2* mutations are associated with ibrutinib resistance, their frequency and relevance to progression are not fully understood. In this multicenter retrospective observational study, we analyzed 98 patients with CLL treated with ibrutinib (49 relapsing after an initial response and 49 still responding after ≥1 year of continuous treatment) using a next-generation sequencing (NGS) panel (1% sensitivity) comprising 13 CLL-relevant genes including *BTK* and *PLCG2*. *BTK* hotspot mutations were validated by droplet digital PCR (ddPCR) (0.1% sensitivity). By integrating NGS and ddPCR results, 32/49 relapsing cases (65%) carried at least 1 hotspot *BTK* mutation and/or *PLCG2* mutation(s); in 6/32, *BTK* mutations were only detected by ddPCR [variant allele frequency (VAF) 0.1-1.2%]. *BTK/PLCG2* mutations were also identified in 6/49 responding patients (12%; 5/6 VAF <10%), of whom 2 progressed at later time points. Among the relapsing patients, the *BTK*-mutated (BTK^{mut}) group was enriched for *EGR2* mutations, while *BTK*-wildtype (BTK^{wt}) cases more frequently displayed *BIRC3* and *NFKBIE* mutations. Using an extended capture-based panel, only *BRAF* and *IKZF3* mutations showed a predominance in relapsing cases, who were enriched for del(8p) (n=11; 3 BTK^{wt}). Finally, no difference in *TP53* mutation burden was observed between BTK^{mut} versus BTK^{wt} relapsing cases, and ibrutinib treatment did not appear to favor selection of *TP53*-aberrant clones. In conclusion, we show that *BTK/PLCG2* mutations were absent in a substantial fraction (35%) of a real-world cohort failing ibrutinib, and propose additional mechanisms contributing to resistance.

Introduction

The first-in-class Bruton tyrosine kinase (BTK) inhibitor ibrutinib covalently binds to BTK,[2,3] and has demonstrated efficacy in both treatment-naïve and relapsed/refractory CLL[4-7]. Although the majority of patients with CLL obtain long-lasting responses, three main reasons for ibrutinib discontinuation have emerged: intolerance (~25% of patients), and, particularly among relapsed/refractory patients, Richter transformation (10%), and CLL progression (~20%).[8,9] Several studies have identified *BTK* and/or *PLCG2* gene mutations in the majority (up to 100%) of patients with CLL relapsing on ibrutinib[10-13], even several months prior to clinical relapse[10,13]. Mutations preferentially occured at the cysteine 481 residue resulting in the replacement of cysteine by serine (p.C481S) or arginine (p.C481R). Mutations at this site lead to abrogation of the covalent binding of ibrutinib, with only transient inhibition of the mutant protein.[10,11] In contrast, multiple, though less frequent, mutations within the downstream signaling molecule PLCG2 usually result in a gain-of-function, promoting B cell receptor (BcR) signaling despite BTK inhibition[14,10,11]. Additional mechanisms of resistance to ibrutinib have been proposed, such as the loss of TRAIL-R expression, due to del(8p),[15,16,17] whereas mutations of individual genes (e.g. *EIF2AK3, EP300, KMT2D*)[15] have been occasionally reported.

The proportion of CLL cells carrying mutations within the *BTK*/*PLCG2* genes varies considerably, with some cases showing a very low clonal burden, hence challenging their proposed contribution to resistance.[18] Thus, a comprehensive understanding of the prevalence and relevance of these mutations in relation to response to ibrutinib will help better refine the mechanisms driving resistance and identify other potential key driver mutations or pathways. In particular, it remains to be established whether these mutations also occur in patients who continue to respond to ibrutinib. Insight into these issues may aid in the validation of

predictors of relapse to assist treatment decisions, and in the design of novel treatment modalities to ultimately prevent relapse and disease progression.

To this end, we designed a multicenter international retrospective study, coordinated by the European Research Initiative on CLL (ERIC), aimed at investigating, in a 'real world' setting, the presence of recurrent gene mutations in *BTK/PLCG2* and other genes of interest by targeted next-generation sequencing (NGS) in patients with CLL failing ibrutinib, and in a cohort of patients who have maintained a response to ibrutinib and remain on therapy for at least 12 months after ibrutinib initiation.

Methods

Patient enrollment and sample collection

Ninety-eight patients with CLL treated with ibrutinib from 21 institutions were included and assigned to one of two groups: relapsed (n=49; patients progressing after an initial response) and responders (n=49; patients who maintained a response to ibrutinib for ≥1 year) (Table 1). Patients in both groups received full-dose ibrutinib without >14 days interruption. Progression and response were defined according to iwCLL 2008 criteria;[19] primary refractory cases and patients with Richter transformation were excluded. Paired samples i.e. at baseline (at the time of treatment initiation) and progression or ≥1 year after therapy initiation, were available for 50 patients (19 relapsed and 31 responders). Informed consent was obtained in accordance with the declaration of Helsinki and ethical approval was granted by local review committees.

A total of 151 samples were analysed, obtained from peripheral blood mononuclear cells (PBMC) (n=143), bone marrow (BM) (n=7) and one baseline sample derived from formalin-fixed paraffin-embedded (FFPE) lymph node tissue. For 3 patients, both BM and PBMC samples obtained at relapse were analyzed.

The fraction of tumor cells by flow cytometry was ≥80% in 79% of all samples in the study. B cells were purified from peripheral blood using a negative-selection immunodensity method (RosetteSep Human B Cells, StemCell Technologies) or from viable frozen PBMCs using a positive-selection method (>95% purity) (EasySep Human CD19 Positive Selection kit II, StemCell Technologies).

Genomic DNA (gDNA) was extracted using Maxwell 16 Blood DNA Purification kit (Promega) for samples with $>1x10^6$ cells; QIAamp DNA Micro kit (Qiagen) for cases with cells numbers ranging from $5x10^4$ to $1x10^6$; NucleoSpin® Tissue XS kit (Macherey-Nagel) for cases with $<5x10^4$ cells. The gDNA concentration was determined using Qubit (ThermoFisher) and integrity was assessed on Agilent 4200 TapeStation (Agilent Technologies).

Next generation sequencing

HaloPlex panel: A previously published custom Agilent HaloPlex High Sensitivity (HS) panel design[20] was modified using the Agilent SureDesign software (https://earray.chem.agilent.com/suredesign/). The custom probes were designed to target the coding exons or hotspot regions of 13 genes of interest in CLL (*ATM, BIRC3, BTK, EGR2, FBXW7, MYD88, NFKBIE, NOTCH1, PLCG2, POT1, SF3B1, TP53* and *XPO1)* (Supplemental Table 1). Libraries were prepared using 50 ng of high-quality gDNA input, following the manufacturer's instructions. Paired-end sequencing (150 bp reads) was performed on a NextSeq instrument (Illumina, USA).

Lymphoid panel: DNA samples were analyzed using a custom-designed, capture-based gene panel, GMS Lymphoid panel (Twist Bioscience), including 252 genes, selected based on their relevance in lymphoid malignancies[21,22]. The panel also included genome-wide

backbone probes for copy-number analysis. Library preparation and sequencing were performed as described in Supplemental Data.

Bioinformatics analysis

HaloPlex panel (see Supplemental Data): FASTQ files were pre-processed by Agilent SureCallTrimmer (v4.0.1) , aligned to the GRCh37 human reference genome using bwa-mem (v0.7.16) and post-processed using Samtools (v1.8). The Agilent LocatIt tool (v4.0.1) was applied for processing of molecular barcode information. Pisces (v5.2.10.49) was used for detection of single nucleotide variants (SNVs) and small insertions/deletions (indels) (1% VAF). Variants were annotated with population variation databases and Cosmic (v85) using VEP[23] (v91) and SnpEFF (v4.3). Pysamstats (v1.1.2) was used for detailed investigation of mutations at codon 481 of the *BTK* gene and at selected *PLCG2* hotspots ("per base" analysis).

Lymphoid panel: BALSAMIC[24] was applied to analyze the FASTQ files and for somatic variant calling (10% VAF) and copy-number aberration (CNA) detection, as described in Supplemental Data.

Droplet digital PCR (ddPCR)

One-hundred-sixteen samples included in the HaloPlex analysis were analyzed with ddPCR with a sensitivity of 0.1% at the *BTK* hotspot C481S (c.1442G>C and c.1441T>A), according to the manufacturer's instructions, using Bio-Rad reagents and equipments (see Supplemental Data).

Statistical analysis

Continuous variables were analyzed using the median and range (minimum, maximum). Categorical variables are presented as percentage of total number of patients with available

information. Correlation of variables with disease outcome were evaluated in univariate analysis with non-parametric tests (Chi-Squared and Fisher Exact test in case of categorical variables, Mann-Whitney and Kruskal-Wallis test in case of continuous variables). Time-to-progression (TTP, time between ibrutinib initiation and documented progression or last follow-up) and overall survival (OS, time between ibrutinib initiation and last follow-up or date of death) were estimated using the Kaplan-Meier Product Limit estimator and Log-rank test.

Results

Patient clinical characteristics

Characteristics of the 98 eligible patients are described in Table 1. The study population was enriched for patients with high-risk features consistent with a heavily pre-treated population (median number of previous therapies 2, range 1-6), with only 17 patients receiving ibrutinib as first-line treatment (13 responders; 4 relapsed). No significant differences between relapsed and responders subgroups were identified, except for a higher percentage of *TP53* mutations in relapsed cases (48% vs 21%, p=0.03). All patients obtained at least a partial response with lymphocytosis (PR-L) on ibrutinib, with those in the relapsed group progressing after a median of 34 months (range, 5-66). The median duration of treatment was 44 months (range, 18-87) in the responders and 36 months (range, 6-68) in the relapsed cases.

Detection of hotspot BTK and PLCG2 mutations by HaloPlex NGS analysis and validation by ddPCR

By applying our standardized bioinformatics pipeline (1% sensitivity), a total of 38 hotspot *BTK* mutations were detected in 24/49 (49%) relapsed patients, with 7/24 (29%) carrying ≥2 hotspot *BTK* mutations (Table 2). The VAF of the individual *BTK* mutations differed considerably (range: 1.8%-79.5%, median 16.8%; not sex normalized). In 6/24 (25%)

patients, *BTK* mutations were present at low-VAF only (<10%), while in 4/24 (16.7%) patients, low- and high-VAF *BTK* mutations co-occurred (Table 2).

Samples from 47/49 (95.9%) relapsed patients were analyzed by ddPCR targeting *BTK* hotspot mutations as well. This analysis confirmed all NGS-detected *BTK* p.C481S mutation(s), with both tests reporting similar VAFs for the majority of mutations (Table 2). Discrepancies were observed in 3 patients (#1, #2, #24), who harbored a p.C481S mutation stemming from 2 different nucleotide substitutions (c.1441T>A and c.1442G>C) with very different VAFs, thus the discordance likely being the result of cross-reactivity in the ddPCR assays due to the strong positivity of the major clone.

The ddPCR assay identified additional *BTK* p.C481S low VAF mutations (range: 0.1-2.4%) in 16 relapsed patients (Table 2). Ten of them carried also a major *BTK* mutated clone identified by both standard NGS and ddPCR analysis and hence were already classed as *BTK* mutated; in 5/11 of these samples the additional *BTK* mutation(s) were confirmed by per base NGS re-analysis (Table 2). In the remaining 6 patients, wildtype by standard NGS analysis (1% sensitivity), the ddPCR assay identified low VAF *BTK* mutations (range: 0.1-1.2%; 5/6 <1%), which were confirmed by per base NGS re-analysis in 4/6 samples. In addition, in 1 of these patients (#29), 2 additional low VAF mutations were retrieved by per base NGS analysis only (Table 2). Samples from BM and PB at the time of relapse were available for 3 patients (#7, #15 and #20). The *BTK* p.C481S mutation was found in both the BM and PBMC sample from all 3 cases (Table 2), with a higher VAF detected in the PBMC in case #7 and #15, and with similar low levels in patient #20, though only detected by either per base NGS analysis or ddPCR in the PBMC sample.

A per base NGS re-analysis was performed for *PLCG2* gene as well at selected hotspots, to detect mutations with VAF <1%. Twelve relapsed patients harboring *BTK* mutation(s) also carried hotspot *PLCG2* mutation(s). In 4 of them (#3, #6, #10 and #20), carrying *BTK*

mutations at low-VAF only (<10%), multiple *PLCG2* mutations with VAFs in the range of 0.2-32.7% were present (Table 2). Amongst the 25/49 (51%) relapsed patients, negative for *BTK* mutations, only 2 cases (#2 and#26) carried hotspot *PLCG2* mutations (Table 2).

Taking all analyses together, 65% of relapsed patients carried at least 1 hotspot mutation in *BTK* and/or *PLCG2*, with 12/30 (40%) carrying *BTK* mutated clone(s) at a VAF <10%, of which 6 at a VAF ≤1.2% (Table 2). No hotspot mutations in *BTK* or *PLCG2* were detected in any of the matched baseline samples.

Only 3/49 (6.1%) responders (#33, #34 and #35) carried the BTK p.C481S substitution at varying allelic frequencies (19.5%, 4.4% and 2.7%, respectively). Two of them (#33 and #34), progressed 6 and 15 months after sampling, respectively, and were also found to harbor *PLCG2* hotspots mutations at low VAFs (Table 2). The third patient (#35) remained in response at last follow-up (10 months post-sampling) and carried no detectable *PLCG2* mutation.

All *BTK* mutations detected by NGS in the 3 responsive patients were confirmed by ddPCR at similar VAFs. In patient #34, the ddPCR assay detected an additional *BTK*-mutated minor subclone (VAF 0.2%) not confirmed by the NGS per base re-analysis; however, another small subclone (VAF 0.7%) was detected by the NGS per base re-analysis (Table 2).

In addition, samples at time point ≥1 year for 43/46 responders, wildtype for *BTK* as assessed by standard NGS analysis, were also analyzed by ddPCR. In 3/43 patients (#36, #37, #38) a p.C481S mutation was found at very low VAF (0.4-1.2%) (Table 2) and was not detected by the NGS per base re-analysis. These 3 patients have maintained a response to ibrutinib at 26, 31 and 33 months post-sampling.

Taking all analyses together, 6/49 responders (12%) carried a hotspot mutation in *BTK/PLCG2*, with 5/6 cases (83%) harboring *BTK* mutations at a VAF <10%.

Finally, 9 mutations with a VAF <10% and lying outside the known hotspot regions within *BTK* (n=4) and *PLCG2* (n=5) were detected, the majority of which had not been reported previously (Table 3). Six of them were found in 5 relapsed patients, all of whom harbored a hotspot mutation in *BTK*/*PLCG2* genes (Table 3), while 3 were observed in responders, with 2 of them having no detectable hotspot mutation (Table 3).

Mutational profiling of the relapsed and responsive cohort

We next investigated the frequency of mutations within the 11 additional genes included in the HaloPlex panel. A total of 415 somatic mutations were detected; no significant difference in the average number of mutations per case in the relapsed vs responsive cohort was observed (4.6 vs 3.9, respectively). The VAF range spanned from 1.4-100%, however, half of all variants were found at allelic frequencies <10% (203/415; 48.9%) (Supplemental Table 2).

Aside from mutations in *BTK* and *PLCG2*, the most frequently mutated genes in the relapsed patients at progression were: *TP53* (29/49, 59%), *ATM* (14/49, 29%), *EGR2* (10/49, 20%), *SF3B1* (9/49, 18%), *NOTCH1* (8/49, 16%) and *BIRC3* (6/49, 12%), and in the responsive patients at ≥1 year sampling after therapy initiation: *TP53* (22/49, 45%), *ATM* (12/49, 24%), *BIRC3* (7/49, 14%), *SF3B1* (6/49, 12%) and *NOTCH1* (6/49, 12%) (Figure 1). Two relapsed and 9 responsive patients (without *BTK/PLCG2* mutations) did not carry mutations in any genes tested. Combining FISH and mutational data, 32/49 (65%) of the relapsed patients displayed *TP53* aberrations compared to 28/49 (57%) of the responsive patients. Along the same lines, 19/49 (39%) patients in the relapsed cohort carried an *ATM* alteration (mutation and/or deletion) *vs* 21/49 (43%) in the responsive cohort.

An asymmetric distribution of mutations in other genes was noted in BTK^{mut} vs BTK^{wt} relapsed patients. Specifically, *EGR2* was mutated in 9/24 BTK^{mut} vs 1/25 BTK^{wt} patients

(p<0.01), while *BIRC3* (n=6; p<0.05) and *NFKBIE* (n=3, p>0.05) mutations were only detected in the BTK^{wt} group (Figure 1). In contrast, *TP53* mutation burden was not significantly different between BTK^{mut} *versus* BTK^{wt} relapsed cases.

In 19 relapsed patients, samples at both baseline and relapse were available. The total number of somatic mutations at baseline was 36 (average: 1.9 range, 1-4), compared to 60 mutations carried by the matched relapse samples (average: 3.2; range, 0-7), the difference being mainly due to the appearance of *BTK/PLCG2* mutations (n=18). In other words, for all other genes analyzed, only a few patients acquired mutations at the relapse *versus* the baseline time point, including two patients who gained *EGR2* mutations at low allelic burdens (#5 and #30) (Supplemental Figure 1; Supplemental Figure 2A). Accordingly, *BIRC3* and *NFKBIE* mutated patients carried mutations at both time points, except for patient #41 who was *NFKBIE* mutated only at baseline with a low allelic burden (Supplemental Figure 2 B,C).

Paired samples (at baseline and at time point ≥1 year) were available for 31 patients in the responsive cohort. The total number of somatic mutations at baseline was 70 (average: 2.3; range, 0-10), compared to 84 mutations detected at time point ≥1 year (average: 2.7; range, 0-11). The frequency of mutated genes in samples at baseline compared to ≥1 year time point was not significantly different (Supplemental Figure 3).

Additional genetic aberrations assessed by the lymphoid panel

To investigate if additional genetic aberrations may be present in relapsed versus responsive patients, we applied a capture-based lymphoid panel and analysed the mutational status of the 239 genes not included in the HaloPlex panel and the genome-wide copy-number status in 104 gDNA samples from 72 patients (38/49 relapsed and 34/49 responsive). We detected recurrent mutations in *ASXL1, BRAF, IKZF3, KRAS, MED12, MGA, RPS15, SPEN*, and *ZFN292*, however only *BRAF,* and potentially *IKZF3,* showed a predominance in relapsed

cases (Supplemental Table 3; Supplemental Figure 4). Considering that occasional patients progressing on ibrutinib[15,16] have displayed *EIF2AK3, EP300,* and *KMT2D* mutations and del(8p), we specifically looked for these aberrations. Only 1 relapsed patient (*BTK*^{mut} by ddPCR only) carried an *EP300* mutation (VAF 47.9%) at relapse, while 2 *KMT2D* mutations (VAF 28.9;65.7%) were retrieved in 1 relapsed *BTK*^{wt} patient at relapse. *EIF2AK3* was wildtype in all patients (Supplemental Table 3). Finally, del(8p) was detected in 13 patients: 11 relapsed, 4 of them *BTK*^{wt} by HaloPlex analysis (1 mutated by ddPCR only), and 2 responsive *BTK*^{wt} patients (Supplemental Table 4).

TP53 clonal dynamics under ibrutinib treatment

Among 19 relapsed patients with paired samples, 7/19 were *TP53* wildtype at both time points (1 of them *BTK*^{mut} by HaloPlex analysis) and 12/19 carried a *TP53* mutation at some point (7/12 with at least 1 *BTK* hotspot mutation detected by HaloPlex analysis). Among the 12 *TP53* mutated patients, 3 showed expansion (n=2) of an existing clone or the appearance (n=1) of a new clone at relapse; 1 showed a reduction of an existing clone; 5 carried a stable mutant clone, at both time points. One patient carried 3 different *TP53* clones and, interestingly, 1 expanded, 1 reduced and 1 appeared at relapse (Figure 2A). In 2 patients the clonal dynamics could not be reliably analysed due to missing CD19^{+} purity data.

Among 31 responsive patients with paired samples, 10/31 were *TP53* wildtype at both time points and 21/31 carried at least one *TP53* mutation at 1 or both time-points. Among the latter, 7 patients showed expansion (n=2) of an existing clone or the appearance (n=5) of 1 or more *TP53* mutations at the time point ≥1 year (VAF<10%); 5 showed a reduction (n=1) or the disappearance (n=4) of existing clones; 4 carried a stable mutant clone, with either high (n=1) or low (n=3) VAF, at both time points (Figure 2B). The remaining 5 patients carried multiple *TP53* mutations at both time points and 4/5 were mainly characterized by clonal

stability or decrease with the appearance of new clones with VAF <10% in 2 of them (Figure 2B).

Correlation of NGS data with clinical outcome in relapsed cases

Among relapsed patients, those with *BTK* and/or *PLCG2* hotspot mutations (n=32, assessed by any method) experienced a longer time to progression than those without mutations (n=17) (median TTP 36 months, range, 5-56 vs 14.5 months, range 5-66, respectively, p=0.053). Clinical indications of progression on ibrutinib did not differ in the 2 subgroups with the most frequent being the presence of lymphadenopathies (22/32 in the *BTK/PLCG2* mutated vs 9/17 in the *BTK/PLCG2* wildtype cases), followed by anemia and/or thrombocytopenia due to bone marrow infiltration (7/32 vs 3/18), splenomegaly (0/31 vs 3/18) and lymphocyte doubling time (3/31 vs 2/18). After a median follow-up of 43 months (8-84), OS in the relapsed cohort was 58 months, without statistically significant difference between the 2 subgroups.

Discussion

In this study, we performed targeted NGS in a real-world cohort of patients with CLL relapsed on or responsive to ibrutinib treatment, to gain further insights into the mechanisms implicated in the emergence of resistance.

We show that up to 65% of patients relapsing on ibrutinib carried at least 1 hotspot *BTK* mutation at the cysteine 481 residue, and/or ≥1 hotspot *PLCG2* mutations, by integrating NGS analysis (1% sensitivity) with more sensitive techniques such as per base NGS analysis and ddPCR (0.1% sensitivity). This prevalence of *BTK/PLCG2* mutations is lower than those reported in most previous studies, where the overall frequency of *BTK* and/or *PLCG2*

mutated relapsed patients (1% VAF cut-off) was up to 100%,[11,12,13,25] hence indicating the existence of alternative mechanisms of resistance. Similar to other cohorts, we found a large proportion (40%) of relapsed *BTK*-mutated cases harboring hotspot mutation(s) with a VAF <10%, including several cases with VAFs bordering 1%, thus questioning how such clones substantially contribute to resistance. This is further complicated by the finding that, also in the responsive cohort, we detected *BTK* mutations in 6 patients (12%), of whom 3 with low VAF (0.4-1.2%). Although 2/6 progressed 6 and 15 months after sampling, the others remained in response (3/4 patients more than 2 years after sampling). For comparison, 6 patients in the relapsed cohort carried similar *BTK* clones at low VAF (0.1-1.5%) but experienced relapse.

Reasonable assumptions could be that the minor mutant clone may exert a dominant effect on the response of the overall wildtype tumor cell population, as suggested for ibrutinib-resistant patients with either CLL[26] or Waldenström Macroglobulinemia,[27] though this would not explain the detection of such mutations in responding patients even after 2 years of follow-up. Alternatively, resistant and mutated cells may reside in a tissue compartment not analyzed or other mechanisms acting independently or co-operatively may exist.

To explore the latter possibility, we characterized our cohort by NGS for other genes associated with disease progression and dismal prognosis[25,28]. Notably, the frequency of *TP53*-mutated clones in both the relapsed and responsive cohorts did not differ significantly. However, there was a striking difference between the two cohorts in terms of clonal size, with the mean VAF% of *TP53* mutant clones being higher in the relapsed *versus* the responsive cohort, at both baseline (57% vs 19%) and relapse/≥1 year time point (59% vs 16%), with almost all *TP53* mutations in the relapsed group having a VAF ≥10%. On the contrary, in the responsive cohort the majority of *TP53* mutations was present at a VAF <10%, at both baseline and at ≥1 year time point. That said, it is interesting to note that

ibrutinib treatment did not appear to favor the selection of *TP53*-aberrant clones even in the relapsed cohort where the majority of clones either remained stable or decreased in size at the time of relapse, similar to the responding cohort. This suggests little if any direct involvement of *TP53* aberrations in the onset of ibrutinib resistance, though the presence of large *TP53*-aberrant clones may give a higher propensity toward clonal evolution due to genomic instability and the occurrence of mutations in other genes or pathways ultimately responsible for drug resistance.

In the relapsed cohort, we detected a biased distribution of other gene mutations in *BTK/PLCG2* mutated vs wildtype subgroups. Interestingly, the transcription factor *EGR2* was almost exclusively mutated in the *BTK*^{mut} relapsed group. EGR2 is activated through ERK phosphorylation upon BcR stimulation, thus suggesting that *EGR2* mutations might lead to a constitutively dysregulated BcR signaling[29], cooperating with the existing *BTK/PLCG2* mutations towards ibrutinib-resistance.

Conversely, *BIRC3* and *NFKBIE* mutations in the relapsed cohort were exclusively detected in the *BTK*^{wt} versus *BTK*^{mut} group (also at baseline), pointing towards an aberrant activation of the canonical/non-canonical NF-κB pathway as a potential mechanism leading to earlier progression and drug escape. *BIRC3* aberrations have been suggested as predictive factors for poor response to chemoimmunotherapy in patients with CLL.[30] Our results potentially extend the role of this gene also in shaping resistance to novel therapies, although in the phase 3 RESONATE study progression-free survival in patients treated with ibrutinib was not affected by baseline *BIRC3* mutational status[31]. Notably, *BIRC3* and/or *NFKBIE* mutations were present also in a minor proportion (14% and 12%) of the responsive patients, respectively. Longer follow-up will be needed to ascertain if the presence of these mutations may associate with future resistance to ibrutinib treatment.[8,9]

Additional genomic aberrations, including del(8p) and mutations in *EIF2AK3, EP300, KMT2D,*[15,16] have been reported in smaller *BTK*^{wt} patient series. By applying a capture-based panel, we confirmed an enrichment of del(8p) in relapsing cases (11 relapsing versus 2 responsive) but with only 3 of them wildtype for *BTK/PLCG2*. Moreover, while recurrent mutations were seen in some other known CLL driver genes, only *BRAF* and *IKZF3* mutations showed a predominance in relapsed cases. In contrast, no clear predilection of mutations in *EIF2AK3, EP300,* and *KMT2D* was observed in relapsing vs responsive cases.

Though the existence of additional genomic aberrations explaining the resistance deserves further studies, it is also intriguing to hypothesize the occurrence of "functional resistance", in the absence of *BTK/PLCG2* mutations, due to either decreased dependence on proximal BcR signaling or to its bypass through the modulation of the functionality of other non-BcR immune pathways.[32] Noteworthy, in a recent study[33], in patients with CLL progressing on idelalisib treatment, *IGF1R* overexpression was associated with progression in the absence of mutations that could explain resistance, highlighting non-genetic mechanisms as causes of secondary resistance.

In conclusion, while we confirm that *BTK*/*PLCG2* mutations are present in patients with CLL relapsing on ibrutinib, more than one third of them do not harbour such mutations even after high sensitivity analyses. We also validate enrichment of del(8p) in relapsing patients, mainly in combination with *BTK* mutations. Importantly, we show that additional genetic mechanisms, in particular aberrant activation of the BcR and NF-κB pathways, may cooperate in determining progression on ibrutinib in some cases. *BTK*/*PLCG2* mutations may appear at low frequency and can be identified also in a small fraction of patients responding to ibrutinib for more than 2 years. As a consequence, though we demonstrate the feasibility of a targeted NGS approach to detect such mutations in real-world, its use should not be applied in routine clinical practice, as currently stated in the international

recommendations, till we accumulate enough evidence on how to guide treatment decisions when a mutation in these (or other) genes are detected prior to clinical progression.

Acknowledgements

This work was in part supported by an unrestricted grant by SUNESIS. This work was in part supported by Associazione Italiana per la Ricerca sul Cancro – AIRC, Milano, Italy (Investigator Grant #20246 and Special Program on Metastatic Disease – 5 per mille #21198); ERA NET TRANSCAN-2 Joint Transnational Call for Proposals: JTC 2014 (project #143 GCH-CLL) and JTC 2016 (project #179 NOVEL), project code (MIS) 5041673; Bando della Ricerca Finalizzata 2018, Ministero della Salute, Roma, Italy (progetto RF-2018-12368231); the Hellenic Precision Medicine Network in Oncology; project ODYSSEAS (Intelligent and Automated Systems for enabling the Design, Simulation and Development of Integrated Processes and Products) implemented under the "Action for the Strategic Development on the Research and Technological Sector", funded by the Operational Programme "Competitiveness, Entrepreneurship and Innovation" (NSRF 2014-2020) and co-financed by Greece and the European Union, with grant agreement no: MIS 5002462"; the Swedish Cancer Society, the Swedish Research Council, the Knut and Alice Wallenberg Foundation, Karolinska Institutet, Karolinska University Hospital, and Radiumhemmets Forskningsfonder, Stockholm; Lion's Cancer Research Foundation, Uppsala; EU's Horizon 2020 research and innovation program under grant agreement No. 739593.

The authors would like to acknowledge Clinical Genomics Uppsala, Science for Life Laboratory, Dept. of Immunology, Genetics and Pathology, Uppsala University, Sweden for providing assistance with ddPCR and analysis.

The authors acknowledge ACRF and Peter MacCallum molecular laboratories and the CLL Global Foundation for their support.

Authorship Contributions

Contribution: S.B. coordinated sample collection, performed NGS experiments, interpreted data and wrote the paper; L.A.S. performed NGS experiments, interpreted data and wrote the paper; V.L. performed bioinformatics analysis and wrote the paper; A.C. analyzed and interpreted clinical data; T.P. and S.W. performed ddPCR experiments and analysis; H.F. and A.S. performed bioinformatic analysis on the lymphoid panel data; A.G. and A.L. prepared and sequenced libraries for the lymphoid panel; F.G. interpreted lymphoid panel data and wrote the paper; P.R. performed sample purification and DNA extraction; L.S. designed the study, coordinated clinical data collection, analyzed and interpreted clinical data and wrote the paper; P.G. and R.R. designed the study, interpreted data and wrote the paper; all authors provided samples and clinical data, and edited and approved the paper for submission.

Conflict of Interest Disclosures: G.G.: advisory board/speaker's bureau: Janssen, Abbvie, AstraZeneca, Beigene. F.F.: honoraria/advisory board: AbbVie, Acerta/AstraZeneca, Janssen-Cilag, BC platforms. O.J.: consultancy: AstraZeneca, Eli Lilly; speaker's bureau: Abbvie, AstraZeneca, Johnson and Johnson. R.W.: meeting sponsorship: AbbVie, Janssen; advisory board: AstraZeneca, Janssen, SecuraBio, Abbvie; speaker: AbbVie, AstraZeneca,

Janssen, Beigene. A.O.: research funding: Beigene, Janssen, AstraZeneca and Gilead. P.B.: honoraria: Abbvie, Gilead, and Janssen; research funding: Gilead. K.S.: honoraria/advisory board: AbbVie, Acerta/AstraZeneca, Gilead, Janssen; research funding: AbbVie, Gilead, Janssen. L.S.: advisory board: AbbVie, AstraZeneca, Janssen. R.R.: honoraria/advisory board: Abbvie, AstraZeneca, Janssen, Illumina and Roche. P.G.: honoraria/advisory board: AbbVie, Acerta/AstraZeneca, Adaptive, ArQule/MSD, BeiGene, CelGene/Juno, Gilead, Janssen, Loxo/Lilly, Sunesis; research funding: AbbVie, Gilead, Janssen, Novartis, Sunesis. The other authors declare no competing financial interests.

References

1. Schiattone L, Ghia P, Scarfo L. The evolving treatment landscape of chronic lymphocytic leukemia. Curr Opin Oncol 2019;31:568-73.
2. Herman SE, Mustafa RZ, Gyamfi JA, et al. Ibrutinib inhibits BCR and NF-kappaB signaling and reduces tumor proliferation in tissue-resident cells of patients with CLL. Blood 2014;123:3286-95.
3. Herman SE, Niemann CU, Farooqui M, et al. Ibrutinib-induced lymphocytosis in patients with chronic lymphocytic leukemia: correlative analyses from a phase II study. Leukemia 2014;28:2188-96.
4. Byrd JC, Furman RR, Coutre SE, et al. Targeting BTK with ibrutinib in relapsed chronic lymphocytic leukemia. N Engl J Med 2013;369:32-42.
5. Byrd JC, Brown JR, O'Brien S, et al. Ibrutinib versus ofatumumab in previously treated chronic lymphoid leukemia. N Engl J Med 2014;371:213-23.
6. Burger JA, Tedeschi A, Barr PM, et al. Ibrutinib as Initial Therapy for Patients with Chronic Lymphocytic Leukemia. N Engl J Med 2015;373:2425-37.
7. O'Brien S, Furman RR, Coutre SE, et al. Ibrutinib as initial therapy for elderly patients with chronic lymphocytic leukaemia or small lymphocytic lymphoma: an open-label, multicentre, phase 1b/2 trial. Lancet Oncol 2014;15:48-58.
8. Jain P, Keating M, Wierda W, et al. Outcomes of patients with chronic lymphocytic leukemia after discontinuing ibrutinib. Blood 2015;125:2062-7.
9. Maddocks KJ, Ruppert AS, Lozanski G, et al. Etiology of Ibrutinib Therapy Discontinuation and Outcomes in Patients With Chronic Lymphocytic Leukemia. JAMA Oncol 2015;1:80-7.
10. Woyach JA, Furman RR, Liu TM, et al. Resistance mechanisms for the Bruton's tyrosine kinase inhibitor ibrutinib. N Engl J Med 2014;370:2286-94.
11. Ahn IE, Underbayev C, Albitar A, et al. Clonal evolution leading to ibrutinib resistance in chronic lymphocytic leukemia. Blood 2017;129:1469-79.
12. Woyach JA, Ruppert AS, Guinn D, et al. BTK(C481S)-Mediated Resistance to Ibrutinib in Chronic Lymphocytic Leukemia. J Clin Oncol 2017;35:1437-43.
13. Bödör C, Kotmayer L, László T, et al. Screening and monitoring of the BTK ^{C481S} mutation in a real-world cohort of patients with relapsed/refractory chronic lymphocytic leukaemia during ibrutinib therapy. Br J Haematol 2021;194:355-64.
14. Liu TM, Woyach JA, Zhong Y, et al. Hypermorphic mutation of phospholipase C, gamma2 acquired in ibrutinib-resistant CLL confers BTK independency upon B-cell receptor activation. Blood 2015;126:61-8.
15. Burger JA, Landau DA, Taylor-Weiner A, et al. Clonal evolution in patients with chronic lymphocytic leukaemia developing resistance to BTK inhibition. Nat Commun 2016;7:11589.
16. Landau DA, Sun C, Rosebrock D, et al. The evolutionary landscape of chronic lymphocytic leukemia treated with ibrutinib targeted therapy. Nat Commun 2017;8:2185.
17. Kadri S, Lee J, Fitzpatrick C, et al. Clonal evolution underlying leukemia progression and Richter transformation in patients with ibrutinib-relapsed CLL. Blood Adv 2017;1:715-27.
18. Lampson BL, Brown JR. Are BTK and PLCG2 mutations necessary and sufficient for ibrutinib resistance in chronic lymphocytic leukemia? Expert Rev Hematol 2018;11:185-94.
19. Hallek M, Cheson BD, Catovsky D, et al. Guidelines for the diagnosis and treatment of chronic lymphocytic leukemia: a report from the International Workshop on Chronic Lymphocytic Leukemia updating the National Cancer Institute-Working Group 1996 guidelines. Blood 2008;111:5446-56.

20. Agathangelidis A, Ljungstrom V, Scarfo L, et al. Highly similar genomic landscapes in monoclonal B-cell lymphocytosis and ultra-stable chronic lymphocytic leukemia with low frequency of driver mutations. Haematologica 2018;103:865-73.
21. Mansouri L, Thorvaldsdottir B, Laidou S, et al. Precision diagnostics in lymphomas - Recent developments and future directions. Semin Cancer Biol 2021;S1044-579X(21)00265-0.
22. Hellström Lindberg E, Cavelier L, Cammenga J, et al. [Precision diagnostics and therapy in hematological malignancies] Lakartidningen 2021;118:20186.
23. McLaren W, Gil L, Hunt SE, et al. The Ensembl Variant Effect Predictor. Genome Biol 2016;17:122.
24. Foroughi-Asl H, Jeggari A, Maqbool K, et al. BALSAMIC: Bioinformatic Analysis Pipeline for Somatic MutatIons in Cancer (v8.2.3). Zenodo. https://doi.org/10.5281/zenodo.5734364
25. Kanagal-Shamanna R, Jain P, Patel KP, et al. Targeted multigene deep sequencing of Bruton tyrosine kinase inhibitor-resistant chronic lymphocytic leukemia with disease progression and Richter transformation. Cancer 2019;125:559-74.
26. Lipsky A, Luan D, Chen S, et al. Single-Cell Multi-Omics Reveals Distinct Paths to Survival of Admixed BTKC481 Mutant Vs. Wild-Type Cells in Clinically Progressing Chronic Lymphocytic Leukemia. American Society of Hematology Annual Meeting2020.
27. Chen JG, Liu X, Munshi M, et al. BTK(Cys481Ser) drives ibrutinib resistance via ERK1/2 and protects BTK(wild-type) MYD88-mutated cells by a paracrine mechanism. Blood 2018;131:2047-59.
28. Mansouri L, Sutton LA, Ljungstrom V, et al. Functional loss of IkappaBepsilon leads to NF-kappaB deregulation in aggressive chronic lymphocytic leukemia. J Exp Med 2015;212:833-43.
29. Young E, Noerenberg D, Mansouri L, et al. EGR2 mutations define a new clinically aggressive subgroup of chronic lymphocytic leukemia. Leukemia 2017;31:1547-54.
30. Diop F, Moia R, Favini C, et al. Biological and clinical implications of BIRC3 mutations in chronic lymphocytic leukemia. Haematologica 2020;105:448-56.
31. Byrd JC, Hillmen P, O'Brien S, et al. Long-term follow-up of the RESONATE phase 3 trial of ibrutinib vs ofatumumab. Blood. 2019;133:2031-42.
32. Gounari M, Ntoufa S, Gerousi M, et al. Dichotomous Toll-like receptor responses in chronic lymphocytic leukemia patients under ibrutinib treatment. Leukemia 2019;33:1030-51.
33. Tausch E, Ljungström V, Agathangelidis A, et al. Secondary resistance to idelalisib is characterized by upregulation of *IGF1R* rather than MAPK/ERK pathway mutations. Blood 2022;blood.2021014550.

Table 1. Clinical characteristics of patients included in the study.

Characteristics	**Relapsed cases (n=49)**	**Responders (n=49)**	**Entire cohort (n=98)**	**p-value**
Median age, y (range)	66 (33-86)	68 (46-85)	67 (33-86)	ns
Male:female	32:17	31:18	63:35	ns
Median number of prior therapies	2	1	2	ns
Unmutated IGHV, n (%)	28/35 (80%)	29/41 (70.7%)	57/76 (75%)	ns
del(11q), n (%)	14/45 (31%)	10/44 (22.7%)	24/89 (26.9%)	ns
del(17p), n (%)	21/46 (45.6%)	21/46 (45.6%)	42/92 (45.6%)	ns
TP53 mutation, n (%)	13/27 (48.1%)	8/38 (21%)	21/65 (32.3%)	0.03
TP53 aberrations [del(17p) and/or *TP53* mutations], n (%)	25/46 (54.3%)	23/46 (50%)	48/92 (52.2%)	ns
Best response to ibrutinib				
PR/PR-L	44/49	35/49	79/98	ns
CR	5/49	14/49	19/98	ns
Median	36	44	40	ns

duration of ibrutinib treatment, m (range)	(6-68)	(18-87)	(6-87)	
Follow-up				
Median follow-up, m (range)	43 (8-84)	46 (18-87)	44 (8-87)	ns
Median overall survival (OS), m (95% CI)	58 (36-80)	NR	NR	p<0.001
Dead, n (%)	25 (51%)	5 (10.2%)	30 (30.6%)	p<0.001

PR: partial response; PR-L: partial response with lymphocytosis; CR: complete response; ns: not significant; CI: confidence interval; NR: not reached

Table 2. *BTK* and *PLCG2* hotspot mutations in relapsed and responsive cohorts, assessed by both HaloPlex NGS and ddPCR analysis

NA: not available; ND: not detected; *BTK* hotspots VAFs were not sex normalized

			***BTK* hotspot mutations**					***PLCG2* hotspot mutations**				
Patient ID	**Cohort**	**%CD19+ in sample**	**coding DNA description**	**protein description**	**Standard NGS VAF (%)**	**Per base NGS VAF (%)**	**ddPCR VAF (%)**	**coding DNA description**	**protein description**	**Standard NGS VAF (%)**	**Per base NGS VAF (%)**	**Ti ibr sa (m**
1	Relapsed	99	c.1442G>C	p.C481S	79,5	79,5	85,0	c.3418G>A	p.D1140N	3,9	3,9	
			c.1441T>A	p.C481S	2,6	2,6	11					
			c.1442G>A	p.C481Y	ND	0,5	not tested					
			c.1441T>C	p.C481R	ND	0,3	not tested	c.2977G>T	p.D993Y	ND	0,9	
								c.3422T>A	p.M1141K	ND	0,4	
2	Relapsed	>90	c.1441T>A	p.C481S	53,4	53,7	65	c.2978A>G	p.D993G	7,9	7,8	
			c.1442G>C	p.C481S	12,8	12,8	30,7	c.2977G>T	p.D993Y	4,8	4,8	
3	Relapsed	85	c.1442G>C	p.C481S	2,7	2,7	2,8	c.3418G>A	p.D1140N	ND	0,4	

			BTK hotspot mutations					*PLCG2* hotspot mutations				
Patient ID	**Cohort**	**%CD19+ in sample**	**coding DNA description**	**protein description**	**Standard NGS VAF (%)**	**Per base NGS VAF (%)**	**ddPCR VAF (%)**	**coding DNA description**	**protein description**	**Standard NGS VAF (%)**	**Per base NGS VAF (%)**	**Ti ibr sa (m**
			c.1441T>A	p.C481S	2,4	2,5	2,2	c.3422T>G	p.M1141R	ND	0,3	
4	Relapsed	unknown	c.1441T>C	p.C481R	40,3	40,1	not tested	None	None	NA	NA	
5	Relapsed	>90	c.1442G>C	p.C481S	32,0	32,0	32,7	None	None	NA	NA	
			c.1441T>A	p.C481S	ND	ND	0,9					
6	Relapsed	unknown	c.1442G>C	p.C481S	6,1	6,1	7,1	c.3412_3414del	p.1138_1138del	13,0	13,0	
			c.1441T>A	p.C481S	ND	ND	0,5	c.2543T>G	p.L848R	9,3	9,3	
								c.3422T>A	p.M1141K	2,0	2,0	
								c.3418G>A	p.D1140N	ND	1,0	
								c.3422T>G	p.M1141R	ND	1,0	
7-BM	Relapsed	>95	c.1442G>C	p.C481S	7,1	7,1	8,0	c.2978A>G	p.D993G	ND	0,8	
7-PBMC		>95	c.1442G>C	p.C481S	23,3	23,3	18,2	c.2978A>G	p.D993G	ND	1,3	
8	Relapsed	>95	c.1442G>C	p.C481S	31,2	31,2	29,6	c.3422T>G	p.M1141R	4,0	4,0	
			c.1441T>A	p.C481S	ND	ND	0,3					
9	Relapsed	85	c.1442G>C	p.C481S	33,2	33,2	35,6	None	None	NA	NA	
10	Relapsed	95	c.1442G>C	p.C481S	7,8	7,8	10,0	c.2977G>T	p.D993Y	32,7	32,7	
			c.1441T>A	p.C481S	ND	ND	inconclusive	c.2977G>C	p.D993H	2,0	2,0	
								c.2978A>G	p.D993G	ND	1,3	
								c.3418G>A	p.D1140N	ND	0,8	
11	Relapsed	95	c.1442G>C	p.C481S	42,7	42,8	41,6	c.2535A>T	p.L845F	ND	0,8	
			c.1441T>A	p.C481S	ND	0,8	2,2	c.2977G>C	p.D993H	ND	0,8	
12	Relapsed	94	c.1442G>C	p.C481S	62,5	62,5	62,7	c.2977G>C	p.D993H	ND	0,8	
13	Relapsed	90	c.1442G>C	p.C481S	17,9	17,9	18,0	None	None	NA	NA	
			c.1441T>A	p.C481S	ND	ND	0,2					
14	Relapsed	85	c.1442G>C	p.C481S	5,8	5,8	6,8	None	None	NA	NA	
			c.1441T>A	p.C481S	ND	0,7	1,0					
15-PBMC	Relapsed	70	c.1442G>C	p.C481S	41,9	41,8	43,8	c.2535A>C	p.L845F	NA	0,8	
			c.1441T>A	p.C481S	ND	0,5	0,7	c.2535A>T	p.L845F	NA	0,8	
15-BM		38	c.1442G>C	p.C481S	11,5	11,5	13,2	None	None	NA	NA	
			c.1441T>A	p.C481S	ND	ND	0,1					
16	Relapsed	35	c.1442G>C	p.C481S	3,0	3,0	not tested	None	None	NA	NA	
17	Relapsed	unknown	c.1442G>C	p.C481S	61,6	61,5	66,3	None	None	NA	NA	
			c.1441T>A	p.C481S	ND	ND	0,3					
			c.1442G>A	p.C481Y	ND	0,5	not tested					
18	Relapsed	99	c.1442G>C	p.C481S	15,7	15,7	17,2	c.2535A>T	p.L845F	NA	0,3	
			c.1441T>A	p.C481S	ND	0,1	0,2					
			c.1442G>A	p.C481Y	ND	1,4	not tested					

			***BTK* hotspot mutations**					***PLCG2* hotspot mutations**				
Patient ID	**Cohort**	**%CD19+ in sample**	**coding DNA description**	**protein description**	**Standard NGS VAF (%)**	**Per base NGS VAF (%)**	**ddPCR VAF (%)**	**coding DNA description**	**protein description**	**Standard NGS VAF (%)**	**Per base NGS VAF (%)**	**Ti ibr sar (m**
19	Relapsed	unknown	c.1441T>A	p.C481S	37,9	37,9	50,3	None	None	NA	NA	
			c.1442G>C	p.C481S	23,4	23,4	39,2					
20-BM	Relapsed	66	c.1442G>C	p.C481S	2,3	2,3	2,2	c.3412_3414del	p.1138_1138del	2,7	2,[illegible]	
								c.2535A>C	p.L845F	3,4	3,4	
								c.2535A>T	p.L845F	2,7	2,[illegible]	
			c.1442G>A	p.C481Y	ND	0,2	not tested	c.2977G>C	p.D993H	1,7	1,[illegible]	
								c.1993C>T	p.R665W	ND	0,[illegible]	
								c.2120C>T	p.S707F	ND	0,[illegible]	
								c.3418G>A	p.D1140N	ND	0,[illegible]	
								c.3422T>A	p.M1141K	ND	0,[illegible]	
								c.3422T>G	p.M1141R	ND	0,[illegible]	
20-PBMC		92	c.1442G>C	p.C481S	ND	1,4	1,8	c.3412_3414del	p.1138_1138del	12,7	12,7	
								c.2535A>C	p.L845F	2,5	2,[illegible]	
								c.2535A>T	p.L845F	2,0	2,[illegible]	
								c.2977G>C	p.D993H	1,8	1,[illegible]	
								c.1993C>T	p.R665W	ND	0,[illegible]	
								c.3418G>A	p.D1140N	ND	0,4	
								c.3422T>A	p.M1141K	ND	0,[illegible]	
								c.3422T>G	p.M1141R	ND	0,[illegible]	
21	Relapsed	unknown	c.1441T>C	p.C481R	51,8	51,7	not tested	None	None	NA	NA	
			c.1442G>C	p.C481S	5,5	5,5	7,2					
			c.1441T>A	p.C481S	1,8	1,8	2,7					
			c.1442G>A	p.C481Y	2,8	2,8	not tested					
			c.1443C>A	p.C481*	2,2	2,2	not tested					
22	Relapsed	73	c.1442G>T	p.C481F	33,5	33,5	not tested	None	None	NA	NA	
			c.1442G>C	p.C481S	4,8	4,8	8,6					
23	Relapsed	81	c.1442G>C	p.C481S	79,3	79,3	79,9	None	None	NA	NA	
			c.1441T>A	p.C481S	ND	0,4	2,4					
24	Relapsed	97	c.1441T>A	p.C481S	47,8	47,8	69,2	None	None	NA	NA	
			c.1442G>C	p.C481S	22	22	57,9					
			c.1442G>A	p.C481Y	4,8	4,8	not tested					
			c.1442G>T	p.C481F	4,6	4,6	not tested					
			c.1441T>C	p.C481R	ND	0,8	not tested					
25	Relapsed	unknown	None	None	NA	NA	NA	c.2120C>T	p.S707F	21,2	21,2	

			BTK hotspot mutations					*PLCG2* hotspot mutations				
Patient ID	**Cohort**	**%CD19+ in sample**	**coding DNA description**	**protein description**	**Standard NGS VAF (%)**	**Per base NGS VAF (%)**	**ddPCR VAF (%)**	**coding DNA description**	**protein description**	**Standard NGS VAF (%)**	**Per base NGS VAF (%)**	**Ti ibr sa (m**
								c.3412_3414del	p.1138_1138del	ND	0,2	
26	Relapsed	75	None	None	NA	NA	NA	c.3416A>G	p.E1139G	3	3,6	
27	Relapsed	74	c.1442G>C	p.C481S	ND	1,2	0,8	None	None	NA	NA	
28	Relapsed	18	c.1442G>C	p.C481S	ND	0,3	0,1	None	None	NA	NA	
29	Relapsed	unknown	c.1441T>A	p.C481S	ND	0,9	1,2	None	None	NA	NA	
			c.1442G>C	p.C481S	ND	1,5	ND					
			c.1441T>C	p.C481R	ND	1,3	not tested					
30	Relapsed	75	c.1442G>C	p.C481S	ND	0,1	0,1	None	None	NA	NA	
31	Relapsed	81	c.1442G>C	p.C481S	ND	ND	0,2	None	None	NA	NA	
32	Relapsed	99	c.1442G>C	p.C481S	ND	ND	0,1	None	None	NA	NA	
33	Responsive	unknown	c.1442G>C	p.C481S	19,5	19,5	18,7	c.2977G>C	p.D993H	2,9	2,8	
								c.2535A>C	p.L845F	ND	1,9	
								c.3419A>G	p.D1140G	ND	0,4	
34	Responsive	unknown	c.1442G>C	p.C481S	4,4	4,4	5,4	c.3419A>G	p.D1140G	5,5	5,2	
								c.2535A>T	p.L845F	3,4	2,9	
								c.2535A>C	p.L845F	2,7	2,4	
			c.1442G>A	p.C481Y	ND	0,7	not tested					
			c.1441T>A	p.C481S	ND	ND	0,2					
35	Responsive	98	c.1442G>C	p.C481S	2,7	2,7	2,7	None	None	NA	NA	
36	Responsive	88	c.1442G>C	p.C481S	ND	ND	0,4	None	None	NA	NA	
37	Responsive	89	c.1442G>C	p.C481S	ND	ND	1,2	None	None	NA	NA	
38	Responsive	89	c.1442G>C	p.C481S	ND	ND	0,7	None	None	NA	NA	

ND: not detected

NA: not available

BTK hotspots VAFs were not sex normalized

Table 3: *BTK* and *PLCG2* non-hotspot mutations in relapsed and responsive cohorts, as assessed by targeted NGS analysis

Patient ID	**Cohort**	**Time point**	**Gene**	**coding DNA description**	**protein description**	**protein domain**	**NGS VAF (%)**	**References**	**Other *BTK* hotspot mutations**	**Other *PLCG2* hotspot mutations**
18	Relapsed	relapse	BTK	c.136C>T	p.R46C	PH	2,6	none	yes	no
26	Relapsed	relapse	BTK	c.946A>G	p.T316A	SH2	3,0	Sharma et al. 2016; Kadri et al. 2017; Jones et al. 2017	no	yes

				c.1003G>C	p.V335L	SH2	3,6	none		
34	Responsive	≥1 year	BTK	c.1283C>A	p.A428D	TK	6,0	Wang et al. 2022	yes	yes
7-PBMC	Relapsed	relapse	PLCG2	c.601C>G	p.Q201E	EF	2,7	none	yes	no
1	Relapsed	relapse	PLCG2	c.683T>A	p.F228Y	EF	1,7	none	yes	yes
6	Relapsed	relapse	PLCG2	c.2543T>G	p.L848R	PH	9,3	Landau et al. 2017	yes	yes
60	Responsive	≥1 year	PLCG2	c.846G>C	p.E282D	EF	3,8	none	no	no
83	Responsive	≥1 year	PLCG2	c.3076A>T	p.A1026T	Y	3,2	none	no	no

Figure Legends

Figure 1. Oncoplot displaying the somatic variants detected in the 13 genes analyzed by a HaloPlex HS custom panel in the relapsed and responding cohorts. Illustrated are the distribution of the somatic variants, IGHV mutational status, cytogenetic profile determined by fluorescence in situ hybridization or lymphoid panel (del(8p)), and the mutation frequency of each gene in the relapsed and responding cohorts, respectively. Patient identifiers are indicated across the top row.

Figure 2. *TP53* clonal dynamics in the relapsed and responsive cohorts. (A) *TP53* clonal dynamics in 10 mutated patients of the relapsed cohort. Each patient is represented by a different color. The vertical axis displays the mutation VAF%, corrected according to the % of $CD19^+$ cells in the sample. Two patients were not included in the chart due to missing $CD19^+$ purity data. (B) *TP53* clonal dynamics in 18 mutated patients of the responsive cohort. Each patient is represented by a different color. The vertical axis displays the mutation VAF%, corrected according to the % of $CD19^+$ cells in the sample. Three patients were not included in the chart due to missing $CD19^+$ purity data.

Figure 1

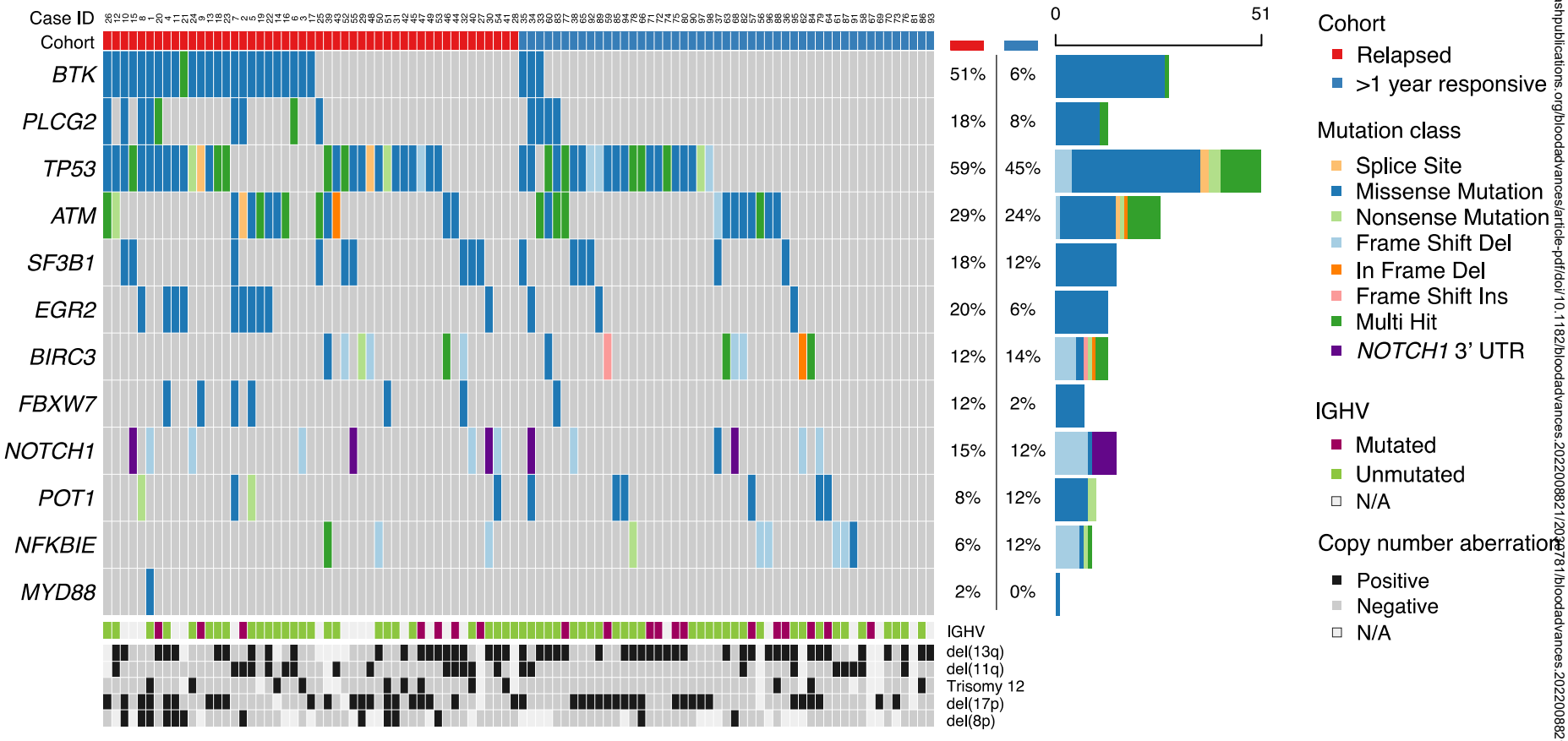

Figure 2